Thickness Dependence of Trapped Magnetic Fields in Machined Bulk MgB_2 Superconductors

Mark D. Ainslie, *Senior Member, IEEE,* and Akiyasu Yamamoto

***Abstract*—MgB_2 in bulk form shows great promise as an inexpensive, lightweight alternative to bulk (RE)-Ba-Cu-O materials to act as trapped field magnets (TFMs), which can replace permanent magnets in applications such as desktop high-field magnet systems and rotating machines. In this paper, we investigate the thickness dependence of the trapped magnetic field in bulk MgB_2 superconductors. Two bulk MgB_2 samples, 20 mm in diameter and 10 mm in thickness, were fabricated using the powder-in-closed-tube (PICT) technique. The trapped field was then measured after field-cooled magnetisation for thicknesses of approximately 20 mm (both bulks stacked), 10 mm (single bulk), and then 7.5, 5, 4, 3, 2, 1.5 and 1 mm, for which the sample was machined down to the designated thickness using an automated-wet-polishing technique. A 2D axisymmetric finite-element model based on the *H*-formulation is used to simulate the experimental results and explain the observed thickness dependence of the trapped field. The numerical results assume a $J_c(B)$ dependence based on the measured characteristics of small specimens taken from the bulk before and after machining. The $J_c(B)$ measurements suggested a degradation of J_c occurred as the bulk was machined thinner and thinner: a decrease in J_c(0 T) of ~35% was observed between the pre- and post-machining specimens. Taking this into account in the models, by assuming a linear reduction in J_c with each machining process, reproduced the experimental results with very good agreement. Consistent trapped field measurements on the top and bottom surfaces suggest this degradation occurred globally, rather than local to the machined surface.**

***Index Terms*—Bulk MgB_2, trapped field magnets, numerical modelling, *H*-formulation, thickness dependence**

I. Introduction

MgB_2 in bulk form shows great promise as an inexpensive, lightweight alternative to bulk (RE)-Ba-Cu-O (where RE = rare earth or yttrium) materials with trapped field capabilities in excess of 3 T, and up to 5.6 T, demonstrated to date [1]–[8]. Magnetised bulk superconductors can act as powerful trapped field magnets (TFMs) and offer significant performance advantages over conventional permanent magnets in a number of applications, including desktop high-field magnet systems and rotating machines [9]. In addition to being inexpensive and lightweight, MgB_2 exhibits a number of additional advantages: a long coherence length, lower anisotropy, strongly-linked supercurrent flow in untextured polycrystalline samples, and the relative ease of fabrication has enabled a number of different processing techniques to be developed [10]–[15]. In this work, the thickness dependence of the trapped magnetic field in bulk MgB_2 superconductors is investigated, experimentally and numerically, to understand the effect of and optimise the geometry in order to maximise their performance as permanent magnet analogues.

Manuscript receipt and acceptance dates will be inserted here. The work of Mark D. Ainslie was supported by the Engineering and Physical Sciences Research Council (EPSRC) Early Career Fellowship EP/P020313/1. This work was also supported by JSPS KAKENHI (JP23246110, JP18H01699 and JP21H01615) and JST CREST (JPMJCR18J4). (Corresponding author: Mark D. Ainslie.)

M. D. Ainslie is with the Bulk Superconductivity Group, Department of Engineering, University of Cambridge, Trumpington Street, Cambridge CB2 1PZ, United Kingdom (e-mail: mark.ainslie@eng.cam.ac.uk).

A. Yamamoto is with the Department of Applied Physics, Tokyo University of Agriculture and Technology, Koganei, Tokyo 184-8588, Japan, and the Materials Research Centre for Element Strategy, Tokyo Institute of Technology, Yokohama, Kanagawa 226-8503, Japan (e-mail: akiyasu@cc.tuat.ac.jp).

Color versions of one or more of the figures in this paper are available online at http://ieeexplore.ieee.org.

Digital Object Identifier will be inserted here upon acceptance.

II. Experimental Details

Two bulk MgB_2 samples, 20 mm in diameter (D) and 10 mm in thickness (t), were fabricated using the powder-in-closed-tube (PICT) technique [3], [4]. The samples were field-cooled (FC) magnetised using a Gifford–McMahon (GM) cryocooler (CRT-HE05-CSFM, Iwatani Gas), under an external field of 6 T generated by a superconducting coil magnet. The samples were initially field-cooled at 5 K, then slowly warmed to 40 K (above the critical temperature, T_c). The trapped field was measured using transversal cryogenic Hall sensors (HGCT-3020, Lake Shore) at the centre of both surfaces for thicknesses of approximately 20 mm (both bulks stacked), 10 mm (single bulk), and then 7.5, 5, 4, 3, 2, 1.5 and 1 mm, for which the sample was machined down to the designated thicknesses using an automated-wet-polishing technique. The automated-wet-polishing was carried out using a Buelher EcoMet™ grinder-polisher, using a low machining speed setting and water as the fluid. Fig. 1 shows photographs of one of the bulk MgB_2 samples under investigation: (a) before machining (t = 10 mm), and (b) the final machined disc (t = 1 mm).

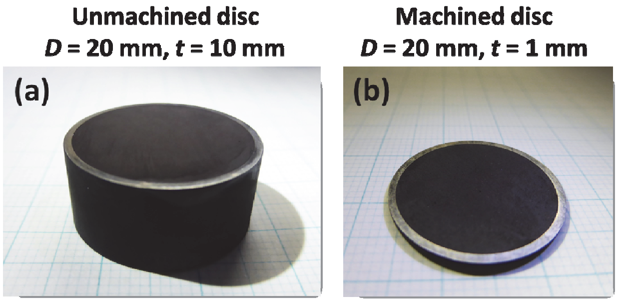

Fig. 1. Photographs of one of the 20 mm-diameter bulk MgB_2 disc samples under investigation, fabricated using the powder-in-closed-tube (PICT) technique: (a) before machining (thickness, t = 10 mm), and (b) the final machined disc (t = 1 mm).

III. Modelling Framework

The model implements the 2D axisymmetric ***H***-formulation [16] and was built in COMSOL Multiphysics using the Magnetic Field Formulation (mfh) interface. The independent variables are the components of the magnetic field strength, $\boldsymbol{H} = [H_r, H_z, 0]$, and the governing equations are derived from Ampere's and Faraday's laws. The current density, $\boldsymbol{J} = [0, 0, J_\varphi]$, and electric field, $\boldsymbol{E} = [0, 0, E_\varphi]$, are parallel to each other, such that $\boldsymbol{E} = \rho\boldsymbol{J}$. The nonlinear resistivity, $\rho(J)$, of the superconductor is simulated using an E-J power law [17], [18]:

$$\boldsymbol{E} = \frac{E_0}{J_c(B)}\left|\frac{\boldsymbol{J}}{J_c(B)}\right|^{n-1}\boldsymbol{J} \tag{1}$$

where E_0 = 1 μV/cm is the electric field criterion, $J_c(B)$ is the magnetic field-dependent critical current density of the superconductor and n (assumed here to be 50) defines the steepness of the transition between the superconducting state and the normal state [19], [20].

The assumed $J_c(B)$ characteristics, shown in Fig. 2 for a temperature T = 20 K, are taken from experimental data for small specimens taken from one of the unmachined bulks and from the final machined bulk. J_c of the small specimens – cut from the centre of the bulks with typical dimensions of 1 × 1 × 0.5 mm^3 – was calculated from the width of the magnetization hysteresis loops measured using a SQUID magnetometer (Quantum Design: MPMS-XL5s). This calculation is based on the extended Bean model using the equation $J_c = 20\Delta M/a(1 - a/3b)$, where $\Delta M = M^+ - M^-$ is the hysteresis loop width, and a and b ($a \le b$) are the dimensions of the rectangular sample [21]. The $J_c(B)$ characteristics are then input into the model using a direct interpolation, as described in [22]–[24]. A mapped mesh, with a fixed element size of 0.33 mm × 0.33 mm, was used to discretize each bulk geometry.

Finally, to simulate the FC magnetisation process, a zero-field-cooling (ZFC) magnetisation process is employed in the simulations by applying and removing a slowly-ramped external magnetic field that is several times larger than the full penetration field of the bulk [16], [25]. All of the modelling results are calculated at z = +0.5 mm above the centre of the top surface of the bulk, taking into account the active region of the Hall sensor in the experiments, and at a time +10 min after the magnetic field is removed to allow for flux creep. Isothermal conditions are assumed because the magnetisation process is slow [10], [16], [25], [26] (and, experimentally, the measured temperature deviation was much less than 1 K); hence, no thermal model is included.

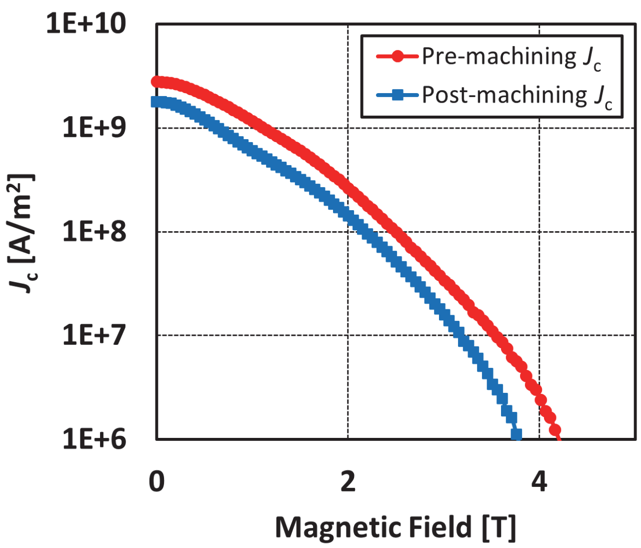

Fig. 2. The assumed $J_c(B$, 20 K) characteristics for the numerical models, based on experimental data for small specimens taken from one of the unmachined bulks ('pre-machining J_c') and from the final machined bulk ('post-machining J_c'). The data is input into the model using a direct interpolation.

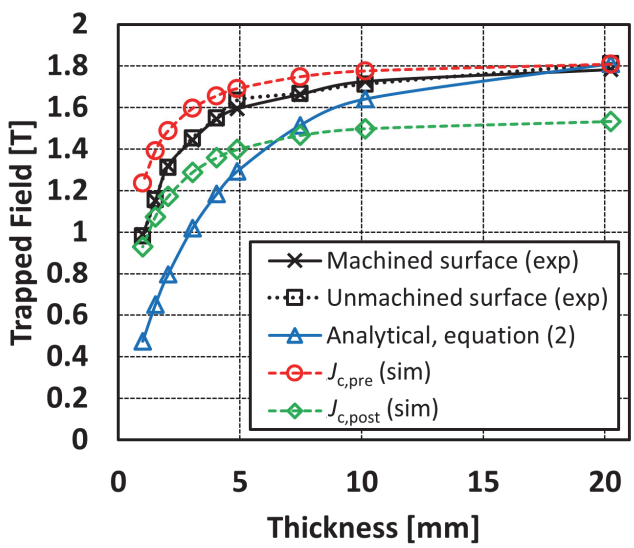

Fig. 3. Comparison of the thickness dependence of the trapped magnetic field between the experimental field-cooled magnetisation results and the modelling results, assuming the pre-machining J_c ($J_{c,pre}$) and post-machining J_c ($J_{c,post}$) separately, for a temperature T = 20 K. Also included are the calculated results from the general analytical formula given by equation (2), based on Bean's critical state model and application of the Biot-Savart law, taking into account the finite thickness of the bulk.

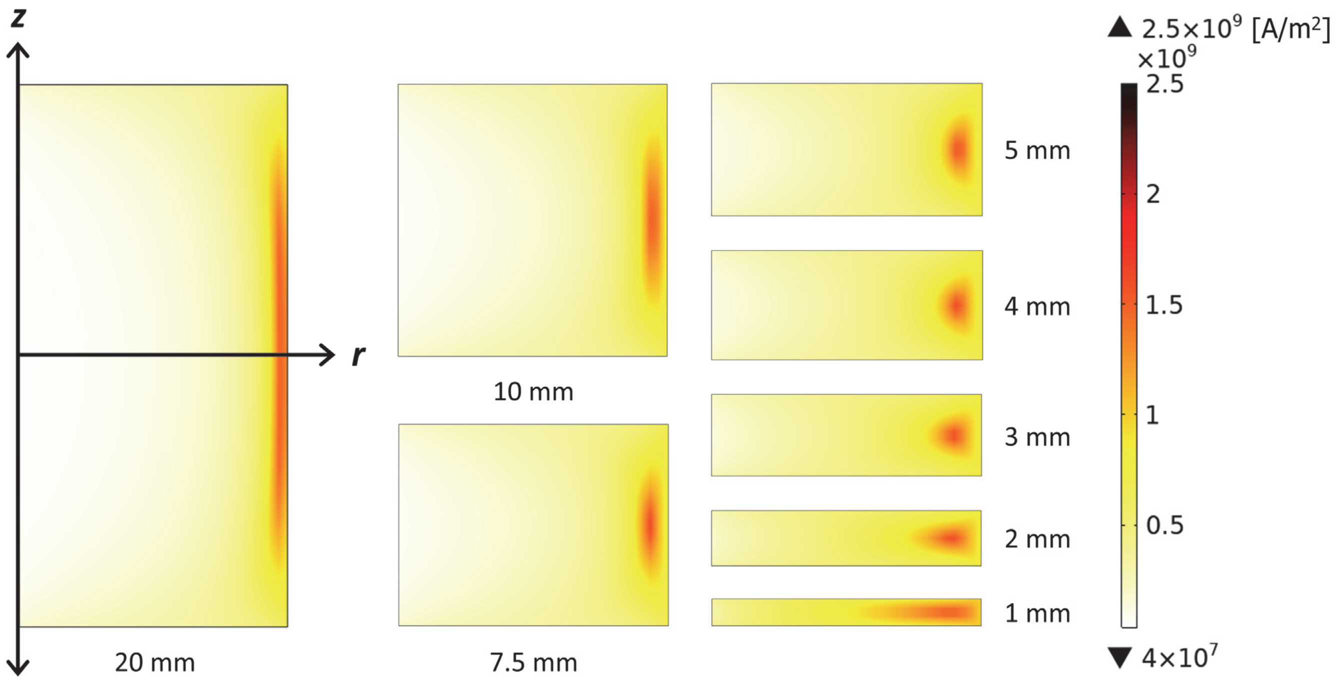

Fig. 4. Comparison of the modelled current density, $|J|$, distributions throughout the cross-section of the MgB_2 bulk as the thickness is varied from 20 to 1 mm assuming the pre-machining J_c ($J_{c,pre}$), for a temperature $T = 20$ K.

IV. Results & Discussion

In Fig. 3, the experimental FC magnetisation results for a temperature $T = 20$ K are compared with the modelling results, firstly assuming the pre-machining J_c ($J_{c,pre}$) and post-machining J_c ($J_{c,post}$) from Fig. 2 separately. Fig. 3 also includes the calculated results from the general analytical formula [27-29], given by (2), based on Bean's critical state model and application of the Biot-Savart law. This equation calculates the magnetic flux density at any height, z, above a superconducting disc of radius, a, carrying an induced, persistent supercurrent of constant critical current density, J_c, taking into account the finite thickness of the bulk, t:

$$B(z) = \frac{\mu_0 J_c}{2}\left[(z+t)\ln\left(\frac{a+\sqrt{a^2+(z+t)^2}}{z+t}\right) - z\cdot\ln\left(\frac{a+\sqrt{a^2+z^2}}{z}\right)\right] \tag{2}$$

Here, J_c is calculated assuming $z = +0.5$ mm (active region of Hall sensor), $t = 20$ mm and $B(+0.5\text{ mm}) = 1.81$ T (from the experimental data), giving $J_c = 3.69 \times 10^8$ A/m^2. This J_c value is then used to calculate B using equation (2) for each thickness. It is obvious that the analytical formula drastically underestimates the trapped field for reducing thicknesses, highlighting the need for numerical models that take into account $J_c(B)$, since J_c varies quite dramatically with B for bulk MgB_2 material as seen in Fig. 2. Thus, in comparison to (RE)-Ba-Cu-O [30] and iron-pnictide [25] bulks, there is a much stronger suppression of J_c for the larger current loops associated with the trapped field of bulks with larger thicknesses. This is evidenced by the current density distributions extracted from the modelling results, as shown in Fig. 4, at the end of the magnetisation process for the $J_{c,pre}$ models. It is clear that as the thickness is reduced, the width over which the highest current density flows increases. Conversely, as the bulk thickness increases, the amount of supercurrent flowing through the cross-section increases, leading to a higher magnetic field within the bulk, and subsequently a stronger suppression of J_c.

The very good agreement for the trapped magnetic field between the experimental results and the modelling results using $J_{c,pre}$ for the unmachined bulk (t = 10, 20 mm) shown in Fig. 3 suggests that the local distribution of superconducting properties inside the MgB_2 bulk sample is quite uniform and the supercurrent flows throughout the whole bulk volume as simulated. Fig. 3 also shows a large discrepancy between the experimental and modelling for most thicknesses, with $J_{c,pre}$ overpredicting the trapped field as the thickness decreases and $J_{c,post}$ underpredicting the trapped field as the thickness increases; however, there is good agreement assuming $J_{c,pre}$ for the unmachined bulk (t = 10, 20 mm) and $J_{c,post}$ for the final thickness (t = 1 mm). This suggests that degradation of J_c occurred as the bulk was machined thinner and thinner: a decrease in J_c(0 T) of ~35% was observed (see Fig. 2) between the pre- and post-machining specimens (a ~0.5 K reduction in T_c was also observed in separate measurements not reported here).

Assuming, for simplicity, that there is a linear reduction in J_c with each machining process, then a new J_c, $J_{c,mod}$, can be defined, such that

$$J_{\text{c,mod}}(B) = J_{\text{c,post}}(B) + \left(J_{\text{c,pre}}(B) - J_{\text{c,post}}(B)\right)\left(\frac{N_{\text{total}} - N_{\text{i}}}{N_{\text{total}}}\right) \quad (3)$$

where N_{total} is the total number of machining processes carried out (here $N_{\text{total}} = 7$) and N_{i} is the i-th machining carried out (i.e., $N_{\text{i}} = 0$ for $t = 10$, 20 mm and $N_{\text{i}} = 1 \ldots 7$ for $t = 7.5 \ldots 1$ mm).

Fig. 5 compares the modelling results assuming $J_{\text{c,mod}}$ with the experimental ones and we find very good agreement between the two. This suggests that the assumption of a gradual reduction in J_{c} with each machining process is a reasonable one. Interestingly, the trapped fields measured on each surface of the bulk (i.e., machined vs unmachined surfaces) did not show any significant difference (< 2% across all thicknesses; see Figs. 3 and 5), suggesting the degradation occurred globally, rather than locally to the machined surface. The exact cause and nature of this degradation warrants further investigation, but is considered to be due to the degradation of grain boundaries caused by mechanical effects and/or penetration of water in the solvent into the porous bulk during the automated-wet-polishing.

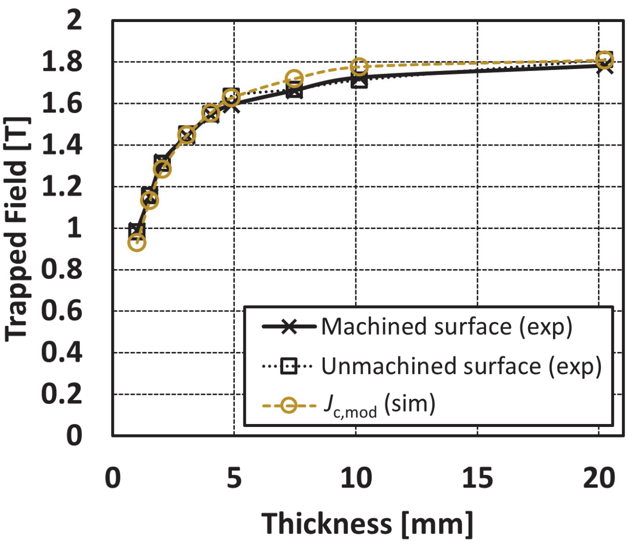

Fig. 5. Comparison of the thickness dependence of the trapped magnetic field between the experimental field-cooled magnetisation results and the modelling results, assuming a linear reduction in J_{c} with each machining process, for a temperature $T = 20$ K.

V. Conclusion

In this paper, the thickness dependence of the trapped magnetic field in bulk MgB_2 superconductors was investigated, experimentally and numerically. A 2D axisymmetric finite-element model based on the $\boldsymbol{H}$-formulation was used to simulate the experimental results for the trapped field in field-cooled bulk MgB_2 samples fabricated using the powder-in-closed-tube (PICT) technique. The trapped field was measured for thicknesses of approximately 20 mm (two bulks stacked), 10 mm (a single bulk), and then 7.5, 5, 4, 3, 2 and 1 mm, for which the sample was machined down to the designated thickness using an automated-wet-polishing technique. The numerical results assumed a $J_{\text{c}}(B)$ dependence based on the measured characteristics of small specimens taken from the bulk before and after machining. The $J_{\text{c}}(B)$ measurements suggested a degradation of J_{c} occurred as the bulk was machined thinner and thinner: a decrease in $J_{\text{c}}(0\text{ T})$ of ~35% was observed between the pre- and post-machining specimens. Taking this into account in the models, by assuming a linear reduction in J_{c} with each machining process, reproduced the experimental results with very good agreement. Consistent trapped field measurements on the top and bottom surfaces suggest this degradation occurred globally, rather than local to the machined surface.

Acknowledgment

The authors would like to thank Mr. S. Sugino and Prof. K. Kishio of the University of Tokyo for their experimental support and fruitful discussions.

Data Statement

Data related to this publication are available at the University of Cambridge data repository [https://doi.org/10.17863/CAM.74840].

References

[1] J. H. Durrell *et al.*, “A trapped field of >3 T in bulk MgB_2 fabricated by uniaxial hot pressing,” *Supercond. Sci. Technol.*, vol. 25, no. 11, 2012, Art. no. 112002.
[2] G. Fuchs *et al.*, “High trapped fields in bulk MgB_2 prepared by hot-pressing of ball-milling precursor powder,” *Supercond. Sci. Technol.*, vol. 26, no. 12, 2013, Art. no. 122002.
[3] A. Yamamoto *et al.*, “Permanent magnet with MgB_2 bulk superconductor,” *Appl. Phys. Lett.*, vol. 105, no. 3, 2014, Art. no. 032601.
[4] S. Sugino *et al.*, “Enhanced trapped field in MgB_2 bulk magnets by tuning grain boundary pinning through milling,” *Supercond. Sci. Technol.*, vol. 28, no. 5, 2015, Art. no. 055016.
[5] K. Berger *et al.*, "High Magnetic Field Generated by Bulk MgB_2 Prepared by Spark Plasma Sintering," *IEEE Trans. Appl. Supercond.*, vol. 26, no. 3, Apr. 2016, Art no. 6801005.
[6] A. G. Bhagurkar *et al.*, “High Trapped Fields in C-doped MgB_2 Bulk Superconductors Fabricated by Infiltration and Growth Process,” *Sci. Rep.*, vol. 8, 2018, Art. no. 13320.
[7] T. Naito, Y. Takahashi, and S. Awaji, “A record-high trapped field of 5.6 T in the stacking of MgB_2/TiB_2 composite bulks prepared by an *in-situ* hot isostatic pressing method,” *Supercond. Sci. Technol.*, vol. 33, no. 12, 2020, Art. no. 125004.
[8] P. Badica *et al.*, “Reproducibility of small $Ge_2C_6H_{10}O_7$-added MgB_2 bulks fabricated by ex situ Spark Plasma Sintering used in compound bulk magnets with a trapped magnetic field above 5 T,” *Sci. Rep.*, vol. 10, 2020, Art. no. 10538.
[9] J. H. Durrell *et al.*, “Bulk superconductors: a roadmap to applications,” *Supercond. Sci. Technol.*, vol. 31, no. 10, 2018, Art. no. 103501.
[10] J. Zou *et al.*, “Numerical modeling and comparison of MgB_2 bulks fabricated by HIP and infiltration growth,” *Supercond. Sci. Technol.*, vol. 28, no. 7, 2015, Art. no. 075009.
[11] G. A. B. Matthews *et al.*, “Design and characterisation of *ex situ* bulk MgB_2 superconductors containing a nanoscale dispersion of artificial pinning centres,” *Supercond. Sci. Technol.*, vol. 33, no. 3, 2020, Art. no. 034006.

[12] L. B. S. Da Silva *et al.*, "Artificial pinning centers in MgB_2 superconducting bulks," *Supercond. Sci. Technol.*, vol. 33, no. 4, 2020, Art. no. 045013.

[13] L. Yang *et al.*, "A novel sintering protocol to enhance the connectivity of *ex situ* MgB_2 bulks in an open system by using Mg vapor," *Supercond. Sci. Technol.*, vol. 33, no. 4, 2020, Art. no. 045006.

[14] M. Jirsa *et al.*, "Flux pinning and microstructure of a bulk MgB_2 doped with diverse additives," *Supercond. Sci. Technol.*, vol. 33, no. 9, 2020, Art. no. 094007.

[15] J. Y. Zhang *et al.*, "The discrepancies in different facets of MgB_2 bulk superconductors prepared under various sintering durations by spark plasma sintering," *Supercond. Sci. Technol.*, vol. 34, no. 4, 2021, Art. no. 045011.

[16] M. D. Ainslie and H. Fujishiro, *Numerical modelling of bulk superconductor magnetisation*. IOP Expanding Physics, Bristol: IOP Publishing, 2020.

[17] C. J. G. Plummer and J. E. Evetts, "Dependence of the shape of the resistive transition on composite inhomogeneity in multifilamentary wires," *IEEE Trans. Magn.*, vol. 23, no. 2, pp. 1179-82, Mar. 1987.

[18] J. Rhyner, "Magnetic properties and AC-losses of superconductors with power law current-voltage characteristics," *Physica C*, vol. 212, no. 3-4, pp. 292-300, 1993.

[19] M. D. Ainslie and H. Fujishiro, "Modelling of bulk superconductor magnetization," *Supercond. Sci. Technol.*, vol. 28, no. 5, 2015, Art. no. 053002.

[20] F. Grilli *et al.*, "Computation of Losses in HTS Under the Action of Varying Magnetic Fields and Currents," *IEEE Trans. Appl. Supercond.*, vol. 24, no. 1, Art. no. 8200433, Feb. 2014.

[21] E. M. Gyorgy *et al*., "Anisotropic critical currents in $Ba_2YCu_3O_7$ analyzed using an extended Bean model," *Appl. Phys. Lett.*, vol. 55, no. 3, pp. 283-5, 1989.

[22] D. Hu *et al.*, "DC characterization and 3D modelling of a triangular, epoxy-impregnated high temperature superconducting coil," *Supercond. Sci. Technol.*, vol. 28, no. 6, 2015, Art. no. 065011.

[23] D. Hu *et al.*, "Modeling and comparison of in-field critical current density anisotropy in high-temperature superconducting (HTS) coated conductors," *IEEE Trans. Appl. Supercond.*, vol. 26, no. 3, Apr. 2016, Art. no. 6600906.

[24] M. D. Ainslie *et al.*, "Enhanced trapped field performance of bulk high-temperature superconductors using split coil, pulsed field magnetization with an iron yoke," *Supercond. Sci. Technol.*, vol. 29, no. 7, 2016, Art. no. 074003.

[25] M. D. Ainslie *et al.*, "Numerical modeling of iron-pnictide bulk superconductor magnetization," *Supercond. Sci. Technol.*, vol. 30, no. 10, 2017, Art. no. 105009.

[26] M. P. Philippe *et al.*, "Influence of soft ferromagnetic sections on the magnetic flux density profile of a large grain, bulk Y-Ba-Cu-O superconductor," *Supercond. Sci. Technol.*, vol. 28, no. 9, 2015, Art. no. 095008.

[27] I-G. Chen *et al*., "Characterization of $YBa_2Cu_3O_7$, including critical current density J_c, by trapped magnetc field," *J. Appl. Phys.*, vol. 72, no. 3, pp. 1013-20, 1992.

[28] Y. Itoh and U. Mizutani, "Pulsed Field Magnetization of Melt-Processed Y-Ba-Cu-O Superconducting Bulk Magnet," *Jpn. J. Appl. Phys.*, vol. 35, no. 4R, pp. 2114-25, 1996.

[29] D. A. Cardwell *et al*., "Round robin tests on large grain melt processed Sm-Ba-Cu-O bulk superconductors," *Supercond. Sci. Technol.*, vol. 18, no. 2, pp. S173-9, 2005.

[30] H. Fukai *et al*., "The effect of geometry on the trapped field in bulk superconductors," *Supercond. Sci. Technol.*, vol. 15, no. 7, pp. 1054-7, 2002.